

THE MOST SUITABLE ALGORITHM FOR INVERTED PENDULUM CONTROL

Peter PÁSTOR

Department of Avionics, Faculty of Aeronautics, Technical University of Košice,
Rampová 7, 041 21 Košice, Slovak Republic, e-mail: pastor_peto@yahoo.com

ABSTRACT

The aim of the paper is to show comparison between three possible realizations of the PID regulator connection. In this case the regulated parameter is deviation from desired vertical position. The structure of the regulator is same like structure of autopilot used in aircraft for pitch angle stabilization. Three different structures of algorithms are described and these structures differ by proportional, integration and derivate gain connection. The goal is to find the most suitable structure for pendulum stabilization. The criteria for the best system selection are system's stability, wide range of stabilized angle, uncomplicated final structure and no overshooting of input's limitations.

Keywords: inverted pendulum, thrust vectoring nozzle, PID regulator, autopilot

1. INTRODUCTION

Inverted pendulum is a typical example of the inherently unstable system and is widely used as benchmark for testing control algorithms (PID controllers, neural networks, fuzzy logic, etc.). This system approximates the dynamics of a rocket immediately after lift-off, or dynamics of a thrust vectored aircraft in unstable flight regimes in low dynamic pressure conditions. The objective of the rocket control problem is to maintain the rocket in a vertical attitude while it accelerates [1]. Angular position of the inverted pendulum is controlled by input force. In this case the controlling force is generated by system of vectored nozzles, where force is directly proportional to nozzle deflection. Position limitation (± 20 deg), rate limitation (± 60 deg/sec) and nozzle dynamic representing by 2nd order transfer function are also considered. The model of the system of the vectored nozzles will be briefly described later. This model is connected with the nonlinear model of the inverted pendulum given by following equations:

$$(M + m) \frac{d^2 x}{dt^2} + ml \frac{d^2 \theta}{dt^2} \cos \theta - ml \left(\frac{d\theta}{dt} \right)^2 = F \quad (1)$$

$$(J + ml^2) \frac{d^2 \theta}{dt^2} = -ml \frac{d^2 x}{dt^2} \cos \theta + mgl \sin \theta \quad (2)$$

where M – mass of the cart, m – mass of the pendulum, l – length to pendulum centre of mass, J – inertia of the pendulum, θ – deviation from vertical position, x – cart position coordinate, g – acceleration of gravity, F – input force. The construction of the model is described in more details in publication [2]. This system will be applied for final nonlinear analyses of the selected controlling system.

Transfer function, given by equation (3) will be utilized for controller design and regulator's parameters setting:

$$\frac{\theta(s)}{U(s)} = \frac{K}{s^2 + \omega_0^2} = \frac{-\frac{l}{J}}{s^2 - g \frac{ml}{J}} = \frac{-1,2815 \cdot 10^{-5}}{s^2 - 1,90836} \quad (3)$$

where K – gain of the system, ω_0 – natural frequency of the system.

This function is easy to analyse and the PID regulator design is also not complicated.

2. 1ST ALGORITHM

The first algorithm structure is described by following control law [3]:

$$F(s) = P[\theta(s) - \theta_z(s)] + sD\theta(s) \quad (4)$$

where $F(s)$ – force applied to the pendulum; $\theta_z(s)$ – desired value of θ angle; P , D – coefficients of the regulator. The structure of this autopilot consists of two loops – outer and inner and is depicted in Fig. 1.

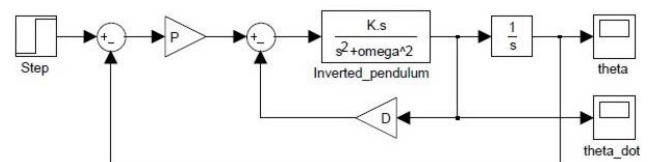


Fig. 1 Structure of the 1st Algorithm

The transfer function of the inner loop is:

$$\frac{Ks}{s^2 + \omega_0^2} \cdot \frac{1}{1 + \frac{KDs}{s^2 + \omega_0^2}} = \frac{Ks}{s^2 + KDs + \omega_0^2} \quad (5)$$

And transfer function of the whole system:

$$\frac{\theta(s)}{\theta_z(s)} = \frac{KP}{s^2 + KDs + (KP + \omega_0^2)} \quad (6)$$

The P , D parameters could be calculated by comparing the denominator of equation (6) with desired denominator shape:

$$s^2 + 2\xi_{SP}\omega_{SP}s + \omega_{SP}^2 \quad (7)$$

From previous formula you can find the similarity with aircraft short period mode and the same criteria for short period damping ζ_{SP} and frequency ω_{SP} are useable for this purpose. The criteria for short period damping and frequency according [4],[5],[6] are:

$$0,35 \leq \zeta_{SP} \leq 1,3; \quad \omega_{SP} \geq 1 \text{ rad / sec}$$

Compare denominator of equation (6) with expression (7): $s^2 + KDs + (KP + \omega_0^2) = s^2 + 2\zeta_{SP}\omega_{SP}s + \omega_{SP}^2$

Coefficient D can be calculated:

$$D = -2\zeta_{SP}\omega_{SP} \frac{J}{l} \quad [kgms^{-1}] \tag{8}$$

And coefficient P:

$$P = -\left(\frac{J}{l}\omega_{SP}^2 + mg\right) \quad [kgms^{-2}] \tag{9}$$

Fig. 2 shows the step response, when input signal is step function with final value: $\pi/10$. This value was approximately calculated from equations (1) and (2). Value of P coefficient is: P= -461049 and D coefficient: D=-312133.

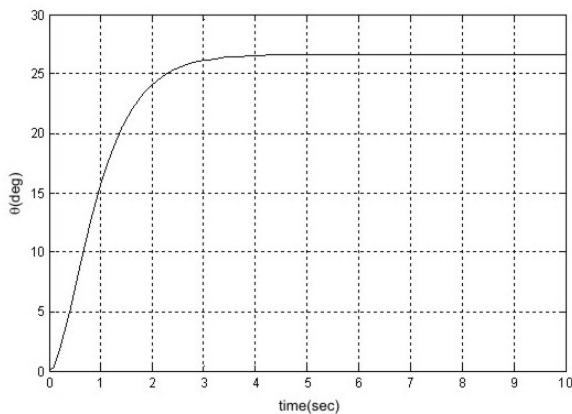


Fig. 2 θ Angle Time Response

You can see from Fig. 3, that the input force in $t=0$ exceeds the limitation and this structure cannot be used for further design.

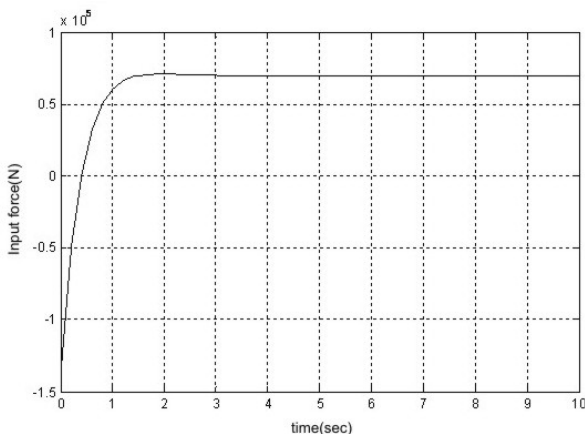


Fig. 3 Input Force Time Response

3. 2ND ALGORITHM

The second algorithm is given by following control law [3]:

$$F(s) = sD\theta(s) + \frac{Ps + I}{s} [\theta(s) - \theta_z(s)] \tag{10}$$

where I – integration coefficient of the PID regulator and meaning of other parameters is same like in equation (4). The structure of the autopilot is depicted in Fig. 4.

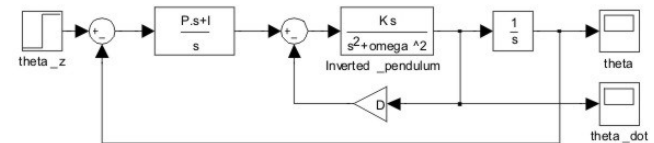


Fig. 4 Structure of the 2nd Algorithm

The model consists also from 2 loops – inner and outer and the transfer function valid for inner loop is given by equation (5). Including outer loop, the final transfer function is:

$$\frac{\theta(s)}{\theta_z(s)} = \frac{KPs + KI}{s^3 + KDs^2 + (KP + \omega_0^2)s + KI} \tag{11}$$

Binomial standard form for 3rd order system describes desired time response [3]: $s^3 + 3\omega_z s^2 + 3\omega_z^2 s + \omega_z^3$, where ω_z is desired value of natural frequency.

The P, I, D coefficients are:

$$P = -\left(3\omega_z^2 \frac{J}{l} + mg\right) \quad [kgms^{-2}] \tag{12}$$

$$I = -\frac{J}{l} \omega_z^3 \quad [kgms^{-3}] \tag{13}$$

$$D = -3\omega_z \frac{J}{l} \quad [kgms^{-1}] \tag{14}$$

The time of regulation can be approximately calculated by using formula:

$$t_r \approx \frac{7}{\omega_z} \quad [\text{sec}] \tag{15}$$

The step response is shown in Fig. 5 and the PID regulator coefficients are: P = - 1085315,8; I = - 624267; D = - 468200.

It can be observed in Fig. 5 – the undesirable overshoot. Try to adjust P, I and D coefficients to eliminate the overshoot. The coefficients for different ω_z value are shown in Table 1.

Table 1 Coefficients for different ω_z value

ω_z	P	I	D
1	-383015,8	-73033	-234100
2	-1085315,8	-624267	-468200
4	-3894515,8	-4994133	-936400

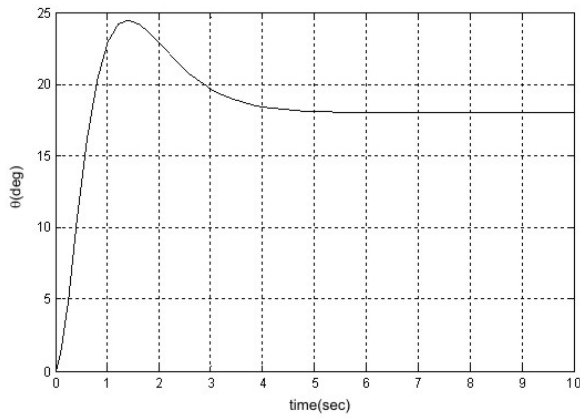


Fig. 5 θ Angle Time Response

It is possible to determine from Fig. 6 the relationship between overshoot and ω_z value. If the ω_z value is increasing, the overshoot is decreasing and vice versa.

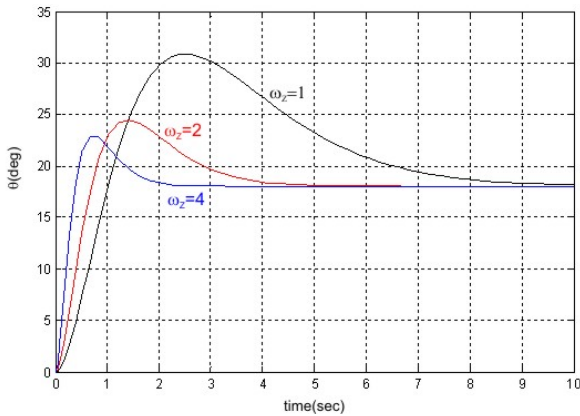


Fig. 6 θ Angle Time Response

You can see in Fig. 7 that input force exceeds limitation again for all coefficients value setting.

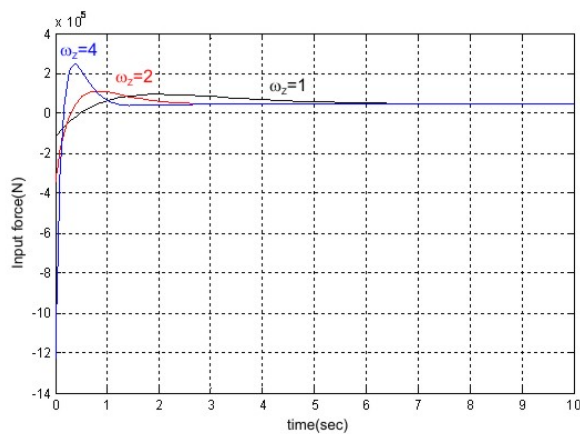


Fig. 7 Input Force Time Response

4. 3RD ALGORITHM

The following control law is valid for third algorithm [3]:

$$sF(s) = s^2 D\theta(s) + sP\theta(s) + I[\theta(s) - \theta_z(s)]$$

Let's divide the previous expression by 1/s:

$$F(s) = sD\theta(s) + P\theta(s) + \frac{I}{s}[\theta(s) - \theta_z(s)] \quad (16)$$

The structure of the autopilot is shown in Fig. 8.

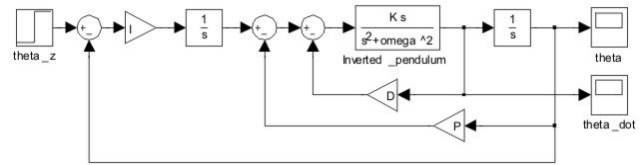


Fig. 8 Structure of the 3rd Algorithm

The structure consists of the three loops – inner, middle and outer. The form of the inner loop is the same like in previous examples and is given by equation (5). The transfer function including middle loop has form:

$$\frac{K}{s^2 + KDs + (KP + \omega_0^2)}$$

And the transfer function of the whole system:

$$\frac{KI}{s^3 + KDs^2 + (KP + \omega_0^2)s + KI} \quad (17)$$

The denominator of equation (17) has the same form like denominator of equation (11), so the same value of P, I, D coefficient are valid. Fig. 9 shows time response to input step function with final value $\pi/10$.

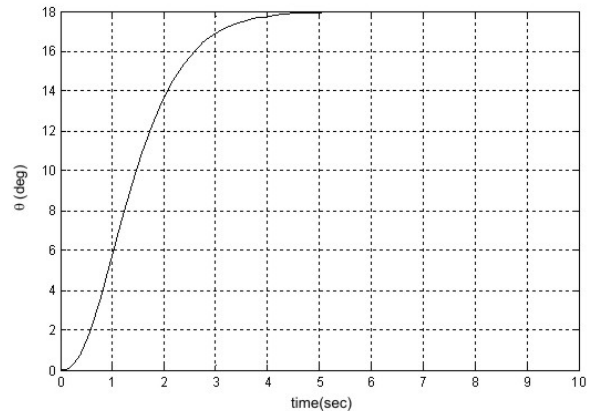


Fig. 9 θ Angle Time Response

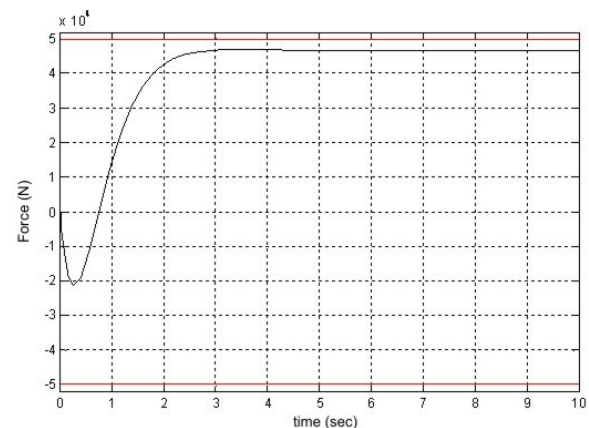


Fig. 10 Input Force Time Response

You can observe in Fig. 10 that input force does not exceed the limitation, which is depicted as red limiting line. This structure is the most suitable for θ angle control, because in previous examples the input force exceeds limited value.

The Bode characteristic of transfer function given by equation (17) is shown in the following figure.

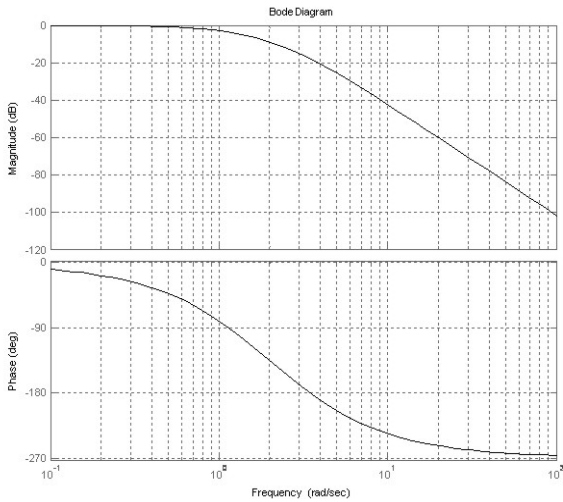


Fig. 11 Bode Characteristic

5. NONLINEAR ANALYSES

The structure for nonlinear analyses consists of two nonlinear models – model of inverted pendulum described by equations (1) (2) and model of thrust vectoring system of aircraft’s engine including dynamic of nozzles given by 2nd order transfer function similar like in publication [4]:

$$\frac{400}{s^2 + 40s + 400}$$

Its deflection is limited ± 20 deg in position and ± 60 deg/sec in rate [1]. Model provides calculation [7] of the summary forces and moments generated by thrust system. In this example only force in pitch control is considered:

$$F(s) = T \cdot \sin \varphi(s) \tag{18}$$

where T is the thrust produced by nozzle and its value is constant during simulation; φ – angle between vectored nozzle deflection and longitudinal axes. Substitute equation (18) into control law (16):

$$T \sin \varphi(s) = sD\theta(s) + P\theta(s) + \frac{I}{s} [\theta(s) - \theta_z(s)] \tag{19}$$

Let’s assume the simplification – for small angle of nozzle deflection (approximately up to 20 deg) is valid: $\sin \varphi(s) = \varphi(s)$. Divide equation (19) by thrust T :

$$\varphi(s) = s \frac{D}{T} \theta(s) + \frac{P}{T} \theta(s) + \frac{I}{T} \cdot \frac{1}{s} [\theta(s) - \theta_z(s)] \tag{20}$$

Equation (20) represents control law for system mention above and shown in Fig. 12.

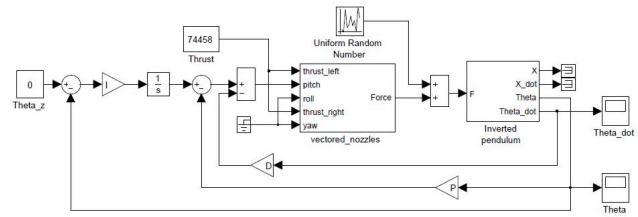


Fig. 12 System for Nonlinear Analyses

New P, I, D values can be calculated by applying equation (20) and assuming that nozzles generated thrust 148 916 N. It is necessary to emphasise, that these parameters are constant only if the thrust of the aircraft is constant. In case the thrust varies during simulation, these parameters have to be adjusted according actual thrust value.

Note the P, I, D values are given as ratio. This is very important fact for practical realization of the similar system with same properties like mention above system.

The system depicted in Fig. 12 was analysed. Fig. 13 shows step response when $\theta_z = 18,8$ deg and this is the maximum value, when pendulum can be stabilized. This limitation can be also calculated from equations (2) and (1) for constant θ value. The motion of the pendulum above this limitation is unstable.

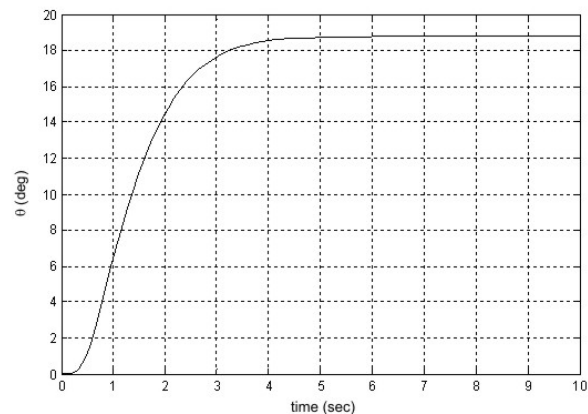


Fig. 13 θ Angle Time Response

If the input is impulse function with period 20 s and pulse width 50% then the maximum θ_z is limited to 16,1 deg. The time response of angle and angular velocity is depicted in the following figures.

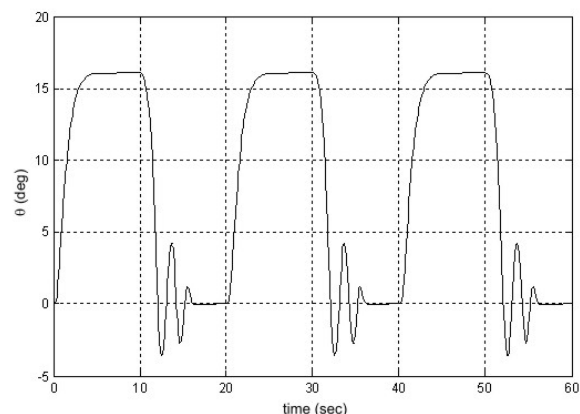


Fig. 14 θ Angle Time Response

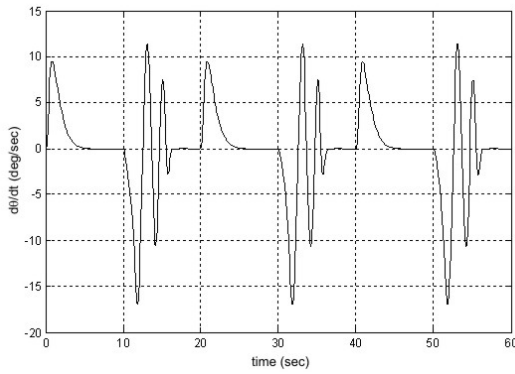


Fig. 15 Angular Velocity Time Response

The following figure shows the response when $\theta_z = 0$ and disturbance random force from region $\pm 50000\text{N}$ is in the input of the inverted pendulum model.

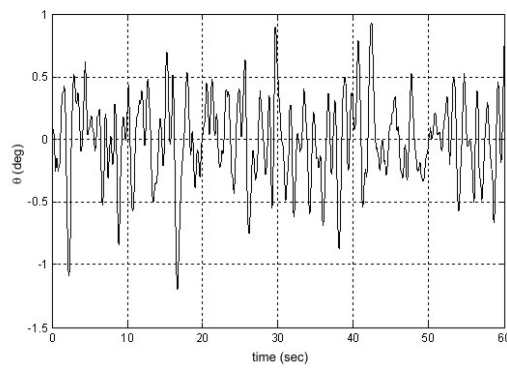


Fig. 16 θ Angle Time Response

Observe also the maximum value of the θ_z as function of input signal frequency in Fig. 17 and in Fig. 18. The condition to determine this value is system stability.

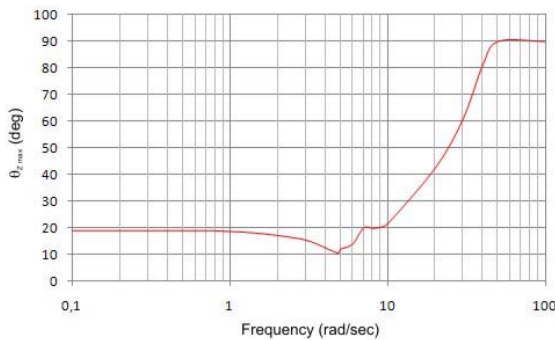


Fig. 17 Maximum θ_z Value

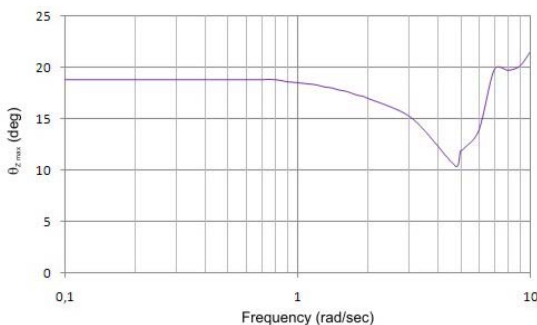


Fig. 18 Maximum θ_z Value in More Details

The maximum disturbance force dependency on the frequency of input force is depicted in Fig. 19.

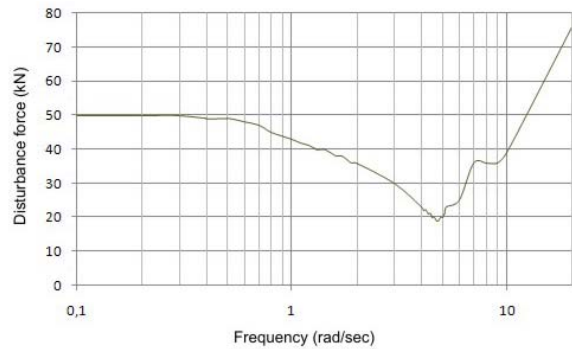


Fig. 19 Disturbance Force

Deviation from desired vertical position is caused by input disturbance. The absolute values of these errors are shown in Fig. 20.

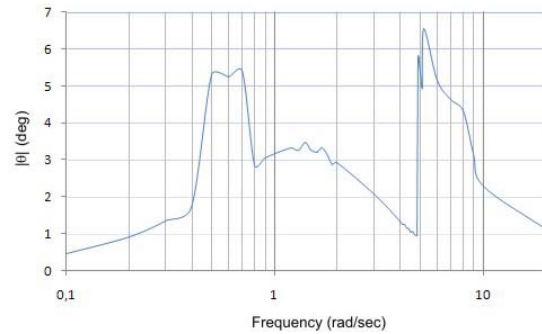


Fig. 20 Absolute Values of Errors

6. CONCLUSIONS

The most suitable structure for inverted pendulum control is structure given by control law (16) and is depicted in Fig. 8. Other structures are not suitable for control, because value of input force exceed the limitation given by vectoring system model. Nonlinear analyses of selected structure also give good results, but other limitations need to be assumed. Envelope of given angle and disturbance force limitation is shown in Fig. 15 and in Fig. 16. Advantage of the PID system control is relatively convenient system design. Disadvantage is small range of controlled angles and sensitivity when frequency of input signal is between 2-7 rad/s. Control system is reliable when these limitations are not exceeded.

REFERENCES

[1] DABNEY, J. – HARMAN, T.: Mastering Simulink. Upper Saddle River: Pearson Prentice Hall, 2004, ISBN 0-13-142477-7.
 [2] WHITE, J. R.: System Dynamics. Online course, http://www.profrwhite.com/system_dynamics/sdyn/s7/s7invp1/s7invp1.html#equations
 [3] LAZAR, T. – ADAMČÍK, F. – LABUN, J.: Modelovanie vlastností a riadenia lietadiel. Faculty of Aeronautics, Technical University of Košice, 2007, ISBN 978 80 8073 8396.

- [4] ADAMS, R. J. – BUFFINGTON, J. M. – SPARKS, A. G. – BANDA, S. S.: Robust Multivariable Flight Control. London: Springer-Verlag, 1994, ISBN 3-540-19906-3. Received November 10, 2010, accepted March 21, 2011
- [5] ROSKAM, J.: Airplane Flight Dynamics and Automatic Flight Controls. Lawrence: Design, Analysis and Research Corporation, 2001, ISBN 1-884885-17-9.
- [6] MIL-STD-1797A, Flying Qualities of Piloted Aircraft, Department of Defence Handbook, 19 December 1997.
- [7] TARANENKO, V. T.: Dinamika samoleta s vertikalnym vzletom i posadkoj. Moskva: Mašinstrojenije, 1978.

BIOGRAPHY

Peter Pástor was born on 6.5.1981. In 2005 he graduated (MSc) with distinction at the department of Avionics of the Faculty of Aeronautics at Technical University in Košice. He is external doctorate student at the department of Avionics of the Faculty of Aeronautics at Technical University in Košice since 2006. His scientific research is focusing on Mathematical modelling of aircraft and aircrafts' engines. In addition, he also investigates questions related with the stabilization of inherently unstable systems.